

This document is confidential and is proprietary to the American Chemical Society and its authors. Do not copy or disclose without written permission. If you have received this item in error, notify the sender and delete all copies.

Multivalent Cation Crosslinking Suppresses Highly Energetic Graphene Oxide's Flammability

Journal:	<i>The Journal of Physical Chemistry</i>
Manuscript ID	jp-2016-13043u.R1
Manuscript Type:	Article
Date Submitted by the Author:	13-Feb-2017
Complete List of Authors:	Turgut, Hulusi; University of Arkansas Fayetteville, Chemistry Tian, Z.; University of Arkansas, Chemistry and Biochemistry Yu, Fengjiao; University of St Andrews, School of Chemistry Zhou, Wuzong; University of St. Andrews , Chemistry

SCHOLARONE™
Manuscripts

Multivalent Cation Crosslinking Suppresses Highly Energetic Graphene Oxide's Flammability

Hulusi Turgut,^{1,2} Z. Ryan Tian^{1,2,3*} Fengjiao Yu,⁴ Wuzong Zhou⁴

AUTHOR ADDRESS

¹Microelectronics/Photonics, University of Arkansas, Fayetteville AR 72701, USA

²Institute of Nanoscience/Engineering, University of Arkansas, Fayetteville AR 72701, USA

³Chemistry/Biochemistry, University of Arkansas, Fayetteville AR 72701, USA

⁴School of Chemistry, University of St Andrews, St Andrews KY16 9ST, UK

Abstract

Graphene oxide (GO), a common intermediate for making graphene-like materials from graphite, was recently found to possess an explosive fire-hazard that can jeopardize the GO's large-scale production and wide applications. This work reports a simple and facile method to cross-link the GO with Al³⁺ cations, in one step, into a freestanding flexible membrane. This inorganic membrane resists in-air burning on an open-flame, at which non-cross-linked GO was burnt out within ~5 seconds. All characterization data suggested that the in-situ "epoxy ring opening" reactions on GO surface facilitated the cross-linking, which elucidated a new mechanism for the generalized inorganic polymerization. With the much improved thermal- and water-stabilities, the cross-linked GO-film can help to advance high-temperature fuel-cells, electronic packaging, etc. as one of the long-sought inorganic polymers known to date.

23 INTRODUCTION

24 Recently, graphene-based new materials have attracted enormous excitement, thanks to
25 their excellent mechanical and electrical properties on top of their highly accessible specific
26 surface area. In search for better and cheaper routes to synthesizing these materials,¹⁻⁷ chemical
27 modification of graphene oxide (GO) is considered the most easily scalable to date⁸⁻¹⁶. This is
28 because, sterically, the modification can easily take place on the oxygenated functional groups
29 (e.g. >O, -OH, -COOH, etc.) that form mostly on the GO edge for exfoliating graphite-layers
30 and dispersing GOs in aqueous and organic solvents. On the GO-surface, the energetic epoxide
31 group was recently found to make the GO highly flammable,¹⁷ and inorganic by-products
32 including potassium and sodium salts (i.e. the residue from the GO synthesis) were shown to
33 contribute significantly to the violent combustibility of the GO in ambient air. This fire-hazard
34 makes the GO to be a dangerous material,¹⁸⁻²¹ especially for the partially reduced GO (or rGO).
35 Hence, a new method should be developed timely for facilely mass-producing flame-retardant
36 and highly thermal-stable GO.²²

37 Herein, we report a new and simple method for mass-producing such non-flammable
38 GO, by cross-linking the GO with Al³⁺ cations in one-step in aqueous solutions at room-
39 temperature. The cross-linked GO (cl-GO) resists combustion in ambient air on open-flame,
40 and shows in addition a greatly improved thermal stability, which ended the abovementioned
41 fire-hazard. This thermally stable cl-GO can be applicable to making devices operational at
42 elevated temperatures (above 120 °C) even in air, such as high-temperature fuel cells, high-
43 temperature coating, thermally stable electronic packaging, to name a few. Our characterization
44 data further suggest that the cross-linked GO inherited all characteristics of ordinary GO except
45 the flammability, and its good dispersibility in water being fine-tunable widely, which greatly
46 expands the new cl-GO's processibility and in turn its wide applicability in industry scale.

49 **EXPERIMENTAL METHODS**

50 **Chemical synthesis of GO.** The GO was prepared by mixing 0.5 g graphite powder (Alfa
51 Aesar, natural, briquetting grade, -200 mesh, 99.9995% metal basis) and 0.5 g NaNO₃ (Alfa
52 Aesar, 98+%) into 23 mL of concentrated H₂SO₄ (BDH Aristar, 95–98 % min) solution, under
53 stirring in an ice bath for 15 minutes. This was followed by adding 4 g of KMnO₄ (J.T.Baker,
54 99% min) gradually under stirring for another 30 minutes in an ice bath, and then transferred
55 into a 40°C water-bath under a stirring for about 90 minutes. The resultant paste was diluted by
56 50 mL deionized water, then stirred for 15 minutes, and then mixed with 6 ml of H₂O₂ (Alfa
57 Aesar 29-32% w/w) and 50 mL distilled/deionized (DDI) water. The resultant product was
58 washed with a copious amount of DDI water and dried at 40°C in air over 24 hours.

60 **Synthesis of aluminum cross-linked graphene oxide (cl-GO).** 300 mg of GO will be
61 dispersed in 100 mL of DDI water under agitation. Separately, 0.2 g of Al(NO₃)₃•9H₂O (EM
62 Science) was added to another 100 mL flask pre-filled with DDI water. The GO dispersion was
63 gradually added into the aluminum nitrate solution, and the resultant cl-GO was stirred for 5
64 minutes at room temperature, then washed with copious amount of DDI water for several times.

66 **Fabrication of GO and cl-GO films.** Same amounts of dispersed cl-GO and GO (1 mg/mL)
67 were used to fabricate films on various substrates such as silicon wafer, polystyrene,
68 polyethylene terephthalate, polytetrafluoroethylene, glass slide, and plastic paraffin film. The
69 best defect-free and durable freestanding GO and Al/GO films were formed on polystyrene
70 substrates using drop-casting methods. After the drop casting on the substrates, films were
71 formed from air-drying over 24 hours at room temperature.

1
2
3 73 **Characterizations.** The GO and cl-GO samples were analysed by means of PHI Versa Probe
4
5 74 Scanning X-ray photoelectron spectroscopy (XPS) Microprobe equipped with dual beam
6
7
8 75 charge neutralization and a monochromatic Al K alpha source (1486 eV). Surveys were
9
10 76 obtained with an 117eV pass energy and 1.0 eV step size, while high resolution spectra were
11
12 77 obtained with 23.5 eV pass energy with 0.1-0.2 eV step size, and with the time of 25 ms per
13
14
15 78 step. For charge correction, 284.8eV was used as the adventitious carbon peak position, and
16
17 79 peak positions were determined by the curve-fitting method.

18
19
20 80 Thermogravimetric Analysis (TGA) tests were performed on TGA Q50 V20.10 Build
21
22 81 36 under N₂ flow, after the samples being heated from room-temperature to 350 °C at the
23
24 82 ramping speed of 15 °C/min. The Differential Scanning Calorimetry (DSC) results were
25
26 83 obtained in a N₂-flow (20 ml/min) on Perkin Elmer Pyris Diamond Differential Scanning
27
28 84 Calorimeter for 5 mg of each sample, first being heated at 50°C for 1 minute then heated up to
29
30 85 300°C at a speed of 10°C /min. The X-ray Powder Diffraction (XRD) patterns were obtained
31
32 86 from a Rigaku MiniFlex II Desktop XRD using monochromatized Cu-K α radiation ($\lambda = 1.5418$
33
34 87 Å) at 30 kV and 15 mA, in the range of 2-theta from 5° to 60° at a speed of 0.1°/min. High
35
36 88 Resolution Scanning Electron Microscopy (SEM) images were obtained using a FEI Nova
37
38 89 Nanolab 200 Duo-Beam Workstation being operated on a 15 kV electron beam. In-house built
39
40 90 Raman spectroscope equipped with 532nm laser source at 3mW was used to obtain the
41
42 91 microRaman spectra. For estimating surface area using the Methylene Blue Absorption
43
44 92 Method, the known masses of GO and cl-GO were separately soaked into an aqueous solution
45
46 93 of metylene blue in 25 ml flasks, then stirred at 400 rpm for 48 hours, then the samples were
47
48 94 centrifuged, and the supernatant's concentration were analysed using Ultraviolet Visible
49
50 95 Spectroscopy (wavelength of 661 nm, U-0080D) for comparison against the original
51
52 96 concentration and knowing the MB molecules being adsorbed. Transmission electron
53
54 97 microscopy (TEM) images were obtained on a JOEL-2011 electron microscope operating at

1
2
3 98 200 kV equipped with an Oxford Link ISIS system for energy-dispersive X-ray spectroscopy
4
5 99 (EDX).
6
7

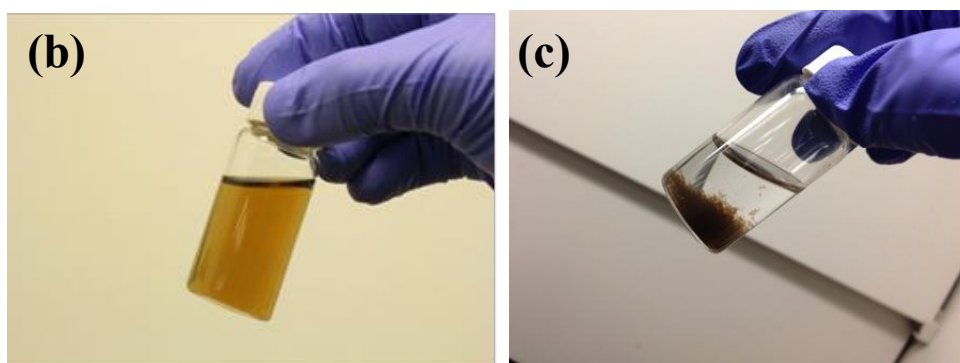
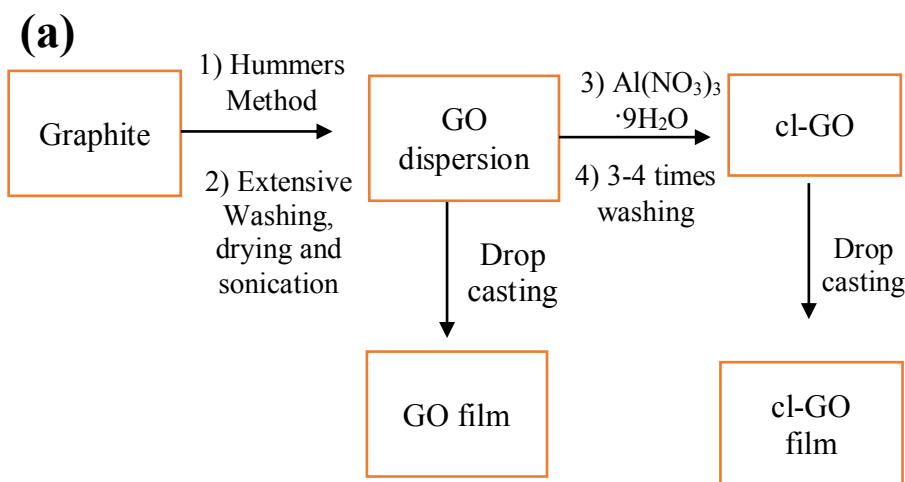
8 100

10 101 **RESULTS/DISCUSSION**

12 102 It was detailed in literature that even an air-drying temperature near 100 °C can trigger
13
14 103 a thermal reduction-decomposition of GO, which is potentially dangerous in large-scale
15
16 104 manufacturing.¹⁷ This is because such a decomposition of GO is as highly exothermic as almost
17
18 105 self-igniting that must be absolutely avoided in any large-scale manufacturing. Moreover, it
19
20 106 was indicated in literature that residual potassium salts, from the GO-synthesis involving
21
22 107 KMnO₄ or K₂S₂O₈, can readily transform to various potassium-containing impurities¹⁸ that can
23
24 108 help turn the GO to the extremely flammable forms. Removing these impurities by employing
25
26 109 filtration or dialysis is time-consuming and costly, because GO-flakes easily clogged the filter-
27
28 110 pores and reduced the water-flow across the filtering media (e.g. anodized aluminum oxide or
29
30 111 AAO). Washing with abundant water was proven troublesome in our experiment, because after
31
32 112 a few washing-cycles the GO started to irreversibly gelatinize which drastically increased the
33
34 113 time and manpower in the follow-up centrifugal separations. Further, both the filtration and
35
36 114 washing still resulted in the GO-flakes with energetic epoxide groups that can make the GO to
37
38 115 be flammable.¹⁷ Thus, an increasing concern has been seriously raised on the fire-hazard of the
39
40 116 GO in especially its large-scale production and applications.¹⁹⁻²¹
41
42
43
44
45
46
47

48 117 Our experiment started from the GO-synthesis (Fig 1a) using a modified Hummer's
49
50 118 method,²² and the resultant GO was washed with water and centrifugation. The GO material
51
52 119 was then dried in an oven, and thereafter exfoliated in DDI water using an ultra-sonication. The
53
54 120 suspension of the exfoliated GO was added into an aqueous solution (1.0% w/w) of Al(NO₃)₃
55
56 121 under a vigorous stirring, in order for the cross-linking to take place instantly at the room-
57
58 122 temperature (Figure 1b-c). This cross-linking was followed by a few times of washing with
59
60 123 DDI water, for further reducing the K-containing impurities' content. Afterwards, 100ml of the

1
2
3 124 GO suspension was centrifuged at 4000 rpm for an hour, and the resultant GO precipitate was
4
5
6 125 collected and then drop-cast on a glass-slide surface to dry into a thin flexible freestanding
7
8 126 membrane about 15-20 microns thick. The cl-GO membrane, together with another similar-
9
10 127 sized GO-film but without the cross-linking, were each exposed to an open-flame from a
11
12
13 128 commercial lighter (burning the butane-fuel) in air.



129
130 **Figure 1.** a) The flowchart for fabricating the GO and cl-GO; b) A GO solution (0.5mg/ml); c)
131 1 minute after the GO being cross-linked in the aqueous solution (1.0 wt%) of $\text{Al}(\text{NO}_3)_3$.

132
133 In chemical science, alkaline earth metal cation is a fairly strong Lewis acid that can
134 form a strong bond on GO, by inducing a ring-opening reaction¹ of the epoxide (a Lewis base)
135 on the GO. The epoxide groups are mainly accountable for the energetic behavior of GO, hence
136 the ring-opening reaction on epoxide group can alter the thermal decomposition kinetics.¹⁷ This
137 motivated us to propose logically and prove in experiment whether this concept's applicability

1
2
3 138 could be expanded to using trivalent metal cations such as Al^{3+} (a much stronger Lewis acid)
4
5 139 to bond with oxygen-containing functional groups including epoxide and carboxylic acid
6
7
8 140 groups in between two adjacent GO-sheets, in either a face-to-face or a shoulder-by-shoulder
9
10 141 manner or even both.

11
12 142 Combustion rapidly propagating made the GO-film to vanish (or gasify) in ~ 5 seconds,
13
14 143 while no combustion (besides reduction) took place on the cl-GO film even after a minute (see
15
16 144 videos in the Supporting Information). Since the open flame is an easily accessible heat source
17
18 145 for GO reduction in scale-up production, we were motivated to further investigate the thermal
19
20 146 behavior for the GO-film and the cl-GO-film.

21
22 147 Thermogravimetric Analysis (TGA) data of GO and cl-GO were compared in Figure
23
24 148 2a. A minor mass-loss for both samples at $100\text{ }^\circ\text{C}$ can be attributed to the desorption of
25
26 149 physisorbed water on the samples, while the major mass-losses at $100\text{ }^\circ\text{C}$ – $300\text{ }^\circ\text{C}$ are due to
27
28 150 the pyrolysis of the oxygen-containing functional groups. The cl-GO exhibited a slower mass-
29
30 151 loss starting around $200\text{ }^\circ\text{C}$, while that of the GO appeared at $125\text{ }^\circ\text{C}$ in a faster rate.

31
32 152 Differential scanning calorimetry (DSC) results (Figure 2b) further suggested that the
33
34 153 GO's thermal decomposition process is much more exothermic than the cl-GO's. Intuitively,
35
36 154 the excessive and abrupt heat-release of GO from the deoxygenation reaction can trigger the
37
38 155 combustion. In contrast, the heat effect of the cl-GO was much smaller. The DSC data, together
39
40 156 with the TGA's, proved the Al^{3+} -crosslinked GO-polymer's thermal-stable nature, which
41
42 157 prompted us to further characterize the GO's and cl-GO's other structural and surface
43
44 158 properties.

45
46 159
47
48 160
49
50 161
51
52 162
53
54
55
56
57
58
59
60
163

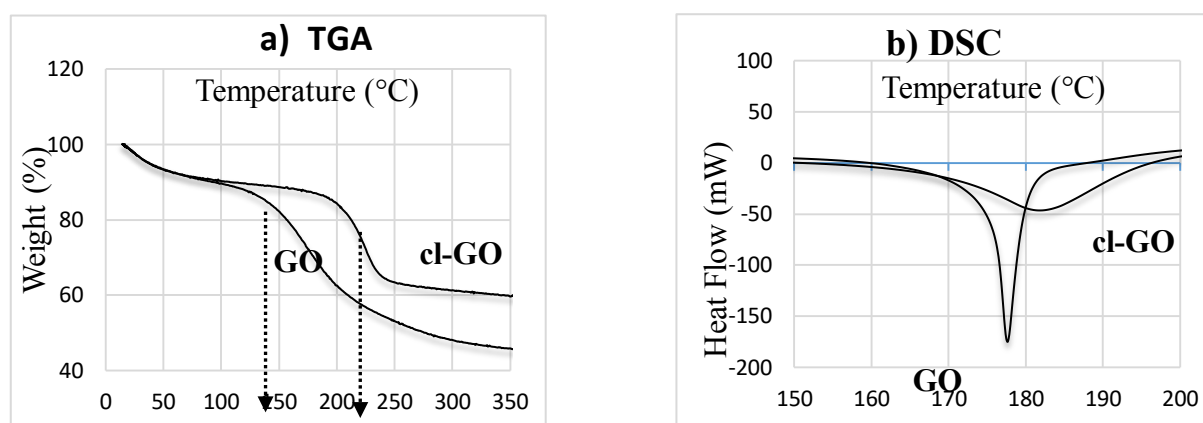


Figure 2. a) TGA curves of GO and cl-GO, from a heating at 15 °C/min under a N₂-flow, showing the mass-loss for cl-GO near 200 °C and that for GO near 125°C. b) DSC curves of GO and cl-GO, from a heating at 10 °C/min under a N₂-flow, showing the heat release (the exothermic peak) of the energetic GO being much greater than that of the thermal-stable cl-GO.

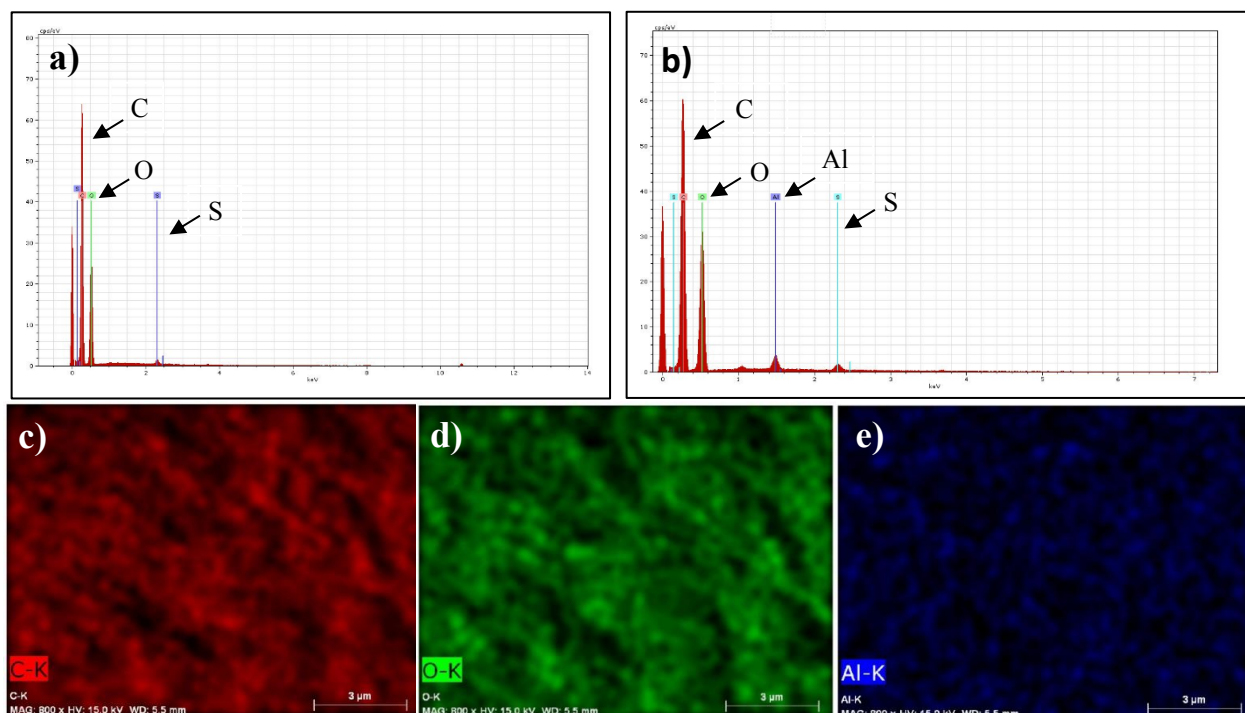
In thermochemistry, GO's decomposition can shift to the more exothermic site due to an increased content of epoxide, and to the more endothermic due to an increased hydroxyl content.¹⁷ The TGA-DSC data suggest that cross-linking Al³⁺ cations on every GO sheets triggered the epoxide ring-opening reaction which decreased epoxide group's content and in turn increased the hydroxyl group content on cl-GO.

For further verifying potassium and sulfur salts' role in the flammability of GO,²¹ a GO-film and a cl-GO film were soaked into a 1.0 wt% aqueous solution of KOH for 5 minutes, and then dried and open-flamed. Again, the GO-film was ignited instantly and disappeared quickly, while cl-GO film was not combusted but turned into a reduced cl-GO. This study further concluded the cl-GO film's nonflammable nature.

An elemental analysis revealed that GO and cl-GO films have sulfur-content of 0.17 at.% and 0.21 at.%, respectively even after being washed extensively with DI water under centrifugation (Figure 3). Surprisingly, as little as 0.42 at% aluminum has led to the GO-polymerization into the cl-GO within a few seconds. Elemental analysis mapping results of cl-

190 GO also showed that Al sparsely distributed along the flakes.

191



192
193 **Figure 3.** Elemental analysis results from a) GO; and b) cl-GO; and the supporting elemental
194 mapping of c) carbon; d) oxygen; e) aluminum.

195
196 The transmission electron microscopic (TEM) image in Figure 4a disclosed the wrinkled
197 nature of graphene sheets. Figure 4b-c further show that the cl-GO sheets are linked up on the
198 GO-edges, and the split ends of two adjacent sheets can be seen in Figure 4c. Under a higher
199 magnification (Figure 4d), a darker middle section is probably due to the existence of a higher
200 content of Al elements.

201

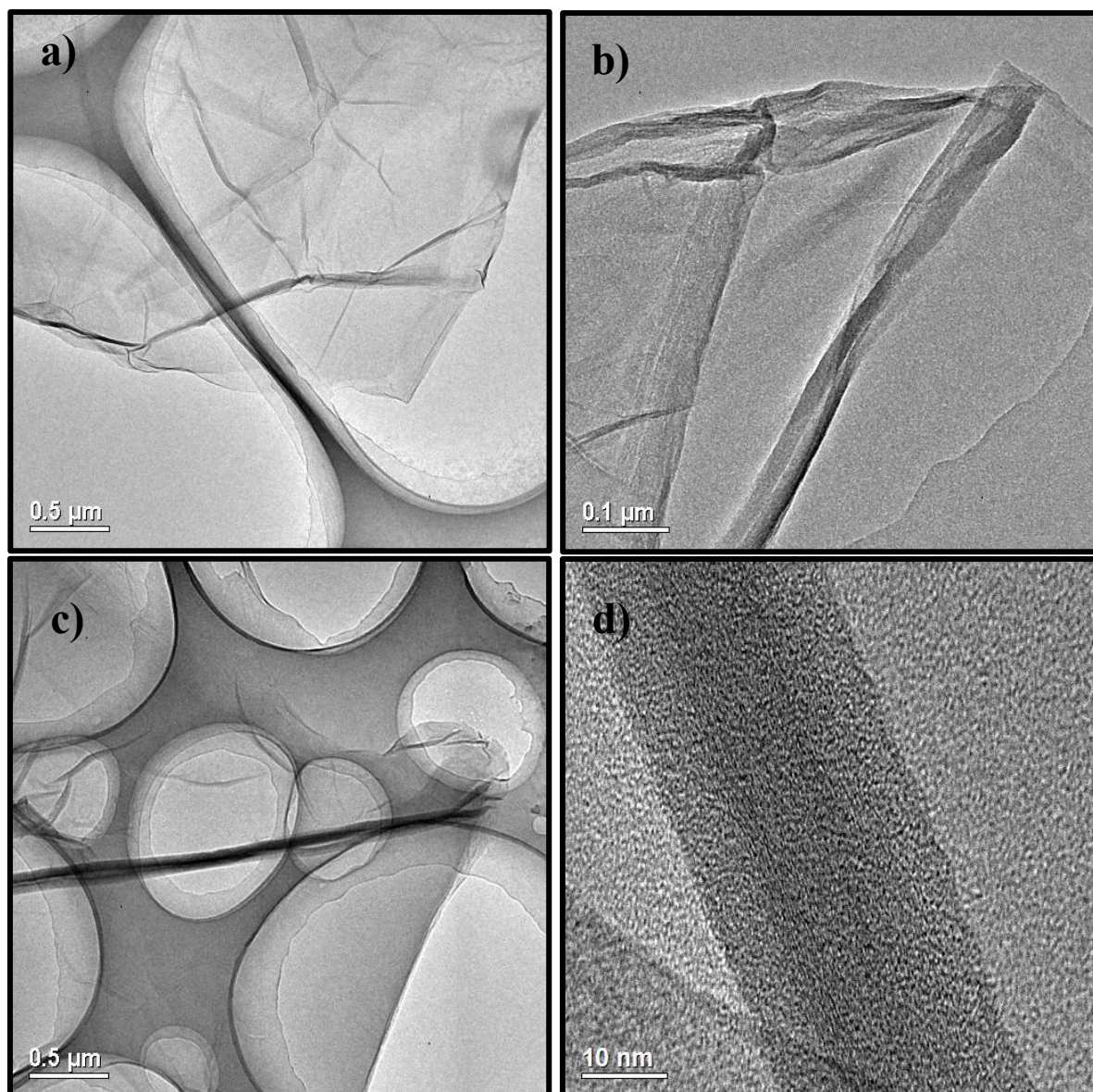


Figure 4. TEM image of cl-GO; a) Characteristic wrinkled GO-sheet; b) and c) Few layers of overlapped and cross-linked GO-sheets; d) High resolution image of the cl-GO sheets.

New reports in literature have indicated that epoxide groups of GO are mainly responsible for GO's high flammability and alteration of these groups can minimize the energetics^{17,18,21}. Thus, we proposed that reducing epoxide groups or all oxygenated functional groups of GO may further minimize the fire hazard. However, it was argued that even the reduced GO (called rGO) can still be extremely flammable due to the residue by-products from the synthesis process of GO¹⁸. On the other hand, the applications can be limited if all

1
2
3 212 oxygenated functional groups are removed in GO. Thus, cl-GO possess unique advantages, by
4
5 213 eliminating high flammability of GO without disturbing major portion of oxygenated groups.
6
7
8 214 The flame resistance and retardancy of cl-GO can be explained by the two major mechanisms:
9
10 215 i) partial pacification of epoxide groups via cross linking them with Al^{3+} cations, ii) shielding
11
12 216 heat propagation between the GO flakes so to result in the cl-GO with superior thermal stability
13
14
15 217 and open flame resistance. One such study reported that upon heating GO the heat transferred
16
17 218 from one highly energetic GO' site to another very rapidly¹⁸, which matches our results from
18
19 219 this work. Our DSC results suggested that when once GO was heated, a thermal decomposition
20
21 220 started to propagate quickly with rapid heat accumulation which is in line with others reports
22
23
24 221 on the same phenomena. However, when cl-GO was heated, much less heat accumulation
25
26 222 between GO flakes prevented the excessive heat accumulation that results in serious fire-
27
28 223 hazard.

29
30
31 224 Surprisingly, some studies in the literature claimed that GO and its derivatives can be
32
33 225 used as a potential flame retardant polymer additive despite its highly energetic structure and
34
35 226 thermal instability²³⁻²⁹. In contrary, a recent review on GO's thermal instability seriously
36
37 227 questioned its use for flame retardant applications and pointed out that GO or contaminated
38
39 228 rGO may behave like a fuel for combustion rather than a flame retardant additive material²¹.
40
41
42 229 The results in the review suggest that there is a strong association between the number of
43
44 230 epoxide groups, the amount of synthesis by-products and GO's flammability. For timely
45
46 231 clarifying the confusion in literature, our cl-GO can be a very strong candidate to resolve the
47
48 232 abovementioned issues with its thermal stability and flame resistant properties.

49
50
51 233 Freestanding flexible films made of GO were demonstrated to be highly promising in
52
53 234 many important applications in solutions,³⁰⁻³⁵ owing to their unique properties such as high
54
55 235 tensile strength, proton conductivity, and durability in water. In literature,³⁶⁻⁴⁰ however,
56
57 236 negatively charged GO was found soluble in water owing to the presence of the residual metal
58
59 237 cations, and Al^{3+} on the anodized aluminum oxide filter was reported to improve the GO sheets

1
2
3 238 mechanical strength.⁴⁰ Hence, in our experiment by sonicating a GO film and a cl-GO film in
4
5 239 water for 10 minutes, the GO film became fragmented while the cl-GO film remained intact,
6
7
8 240 which defined a need to study the cl-Go's unusual microstructure.

9
10 241 The cross-linking was further supported by the Fourier-transform infrared (FT-IR)
11
12 242 spectra (Figure 5a). In comparison with the GO's typical vibrations for C=O (1733 cm⁻¹),
13
14 243 aromatic C=C (1618 cm⁻¹), carbonyl (or carboxyl) C-O (1411 cm⁻¹), epoxy C-O (1226 cm⁻¹),
15
16 244 and alkoxy C-O (1057-1149 cm⁻¹), the cl-GO showed a much lower C=O's intensity. This
17
18 245 suggests that the GO's energetic epoxy groups were reacted with the Al³⁺ cations through the
19
20 246 ring-opening reaction, which decreased the content hence intensity of the epoxy vibration.
21
22
23 247 Moreover, the vibration was slightly "red"-shifted to a lower frequency probably because of
24
25
26 248 the leftover ether-like functional groups that are hard to react with the Al (III) cations.

27
28
29 249 In powder X-ray diffraction (XRD) data (Fig. 5b), the main diffraction peak of the GO
30
31 250 sample appear at 2-theta of 11.4° (a lower d-space), whereas that of cl-GO at 10.39° (a higher
32
33 251 d-space). This difference proves that upon cross-linking, the d-space in between the stacked cl-
34
35 252 GO flakes was increased by the "sandwiched" Al³⁺ cations, from 0.79 nm in GO to 0.85 nm in
36
37
38 253 cl-GO. Thus-increased interlayer spacing is a strong evidence of the intercalating-cross-linking
39
40
41 254 of the Al (III) cations in between the cl-GO flakes.

42
43 255 The epoxide ring-opening of GO-polymerization is suggested by X-ray photoelectron
44
45 256 spectroscopy (XPS) data of C1s signals of the GO and cl-GO samples (Figure 5c-d). The C-O
46
47
48 257 peak is mainly due to the epoxy/ether groups, and the C=O peak due to the carboxyl and ketone
49
50 258 groups. The C-C, C-O and C=O peaks for GO ought to appear at 284.6eV, 286.8eV, and
51
52 259 288.56eV, respectively. The C-C, C-O, and C=O peaks for cl-GO, however, were instead
53
54
55 260 recorded at 284.6eV, 287.0eV, and 288.6eV, respectively. On a much lower intensity, the C-O
56
57
58 261 signal (epoxy/ether peak) of cl-GO significantly shifted upward by 0.2 eV (i.e. more stable or
59
60 262 less energetic), which is in line with the epoxide-ring-opening reaction with Al (III) cations.

263

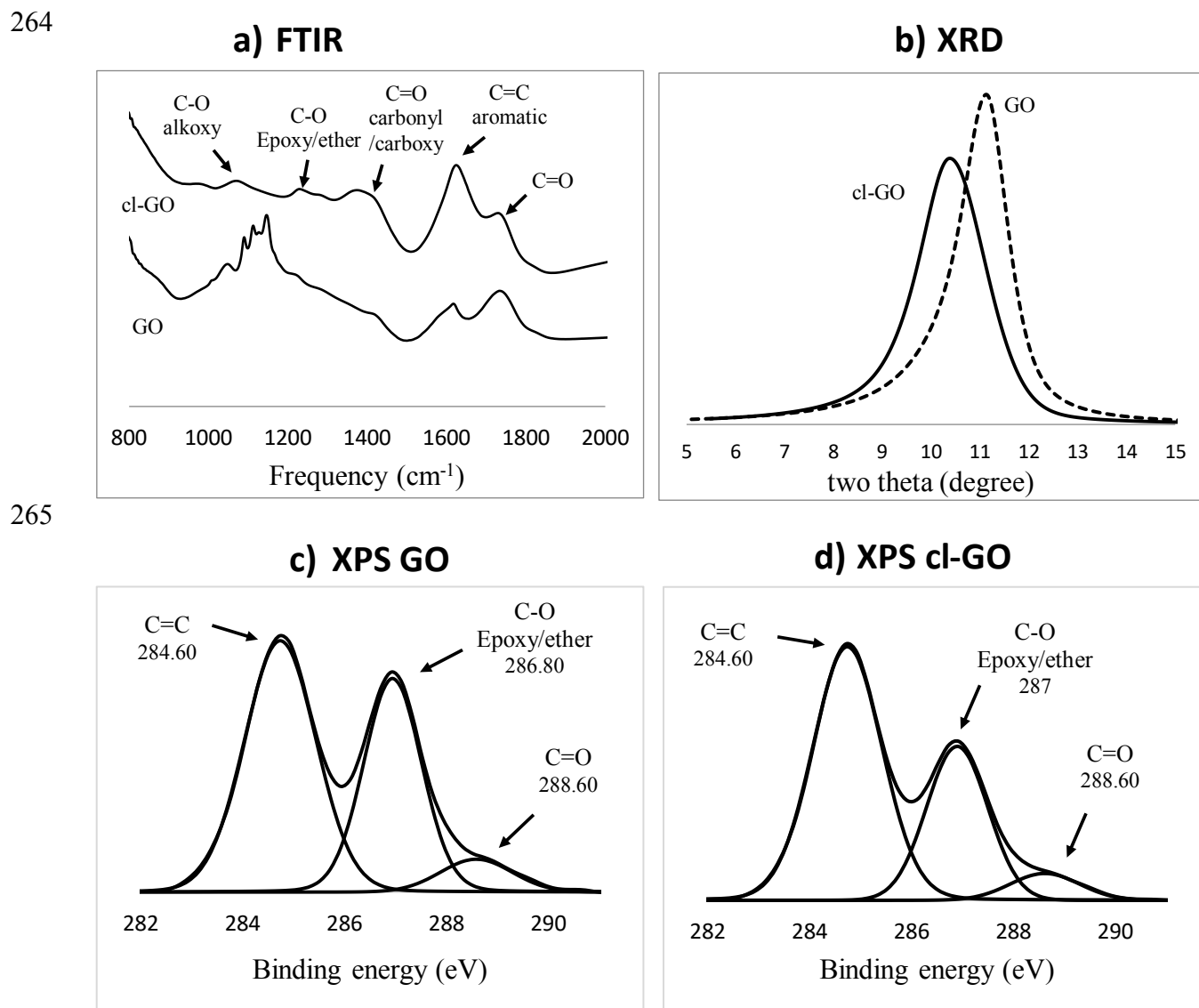
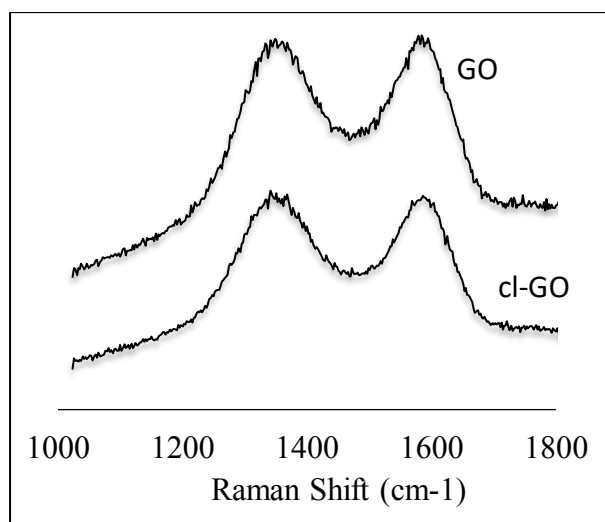


Figure 5. Characterizations of GO and cl-GO. a) FT-IR spectra; b) XRD patterns; c) Deconvoluted XPS spectra of GO; d) cl-GO.

The micro-Raman spectra of GO exhibit two broad peaks at 1593 cm^{-1} and 1355 cm^{-1} corresponding to the G and D bands, respectively (Figure 6). The G peak is associated with the first order E_{2G} mode while the D peak is associated with disordered structure of graphite^{41,42}. It has been consistently reported that removing oxygenated functional groups from GO can result in an increased D/G signal-intensity ratio, because of the defects from the reduction⁴³. Further, the increased D/G signal-intensity ratio has been consistently observed upon reduction of GO,

1
2
3 276 which could be attributed to the enhanced graphitic structure of GO⁴¹⁻⁴⁶. Accordingly, in this
4
5
6 277 study, the cross-linking changed the D/G signal-intensity ratio, from 1.06 in GO to 1.11 in cl-
7
8 278 GO. This slight increase in the D/G signal-intensity ratio of cl-GO suggests that the graphitic
9
10 279 character was slightly increased in the cl-GO upon the cross-linking process.
11
12

13 280



14 281

15 282 **Figure 6.** Micro-Raman spectra of GO and cl-GO.

16 283

17
18
19
20
21
22
23
24
25
26
27
28
29
30 284 In literature,⁴⁷ the methylene blue adsorption method is recommended as a simple and
31
32 285 effective method to estimate graphitic material's surface area, in which each adsorbed
33
34 286 methylene blue's cross-sectional surface area is about 1.35 nm². We, using this method,
35
36 287 estimated the surface area of GO and cl-GO to be 645 and 735 m²/g, respectively. The extra 90
37
38 288 m²/g should be attributed to more methylene blue molecules accessing to the expanded inter-
39
40 289 flake space and the Al³⁺ cations.
41
42
43
44
45
46
47
48
49
50

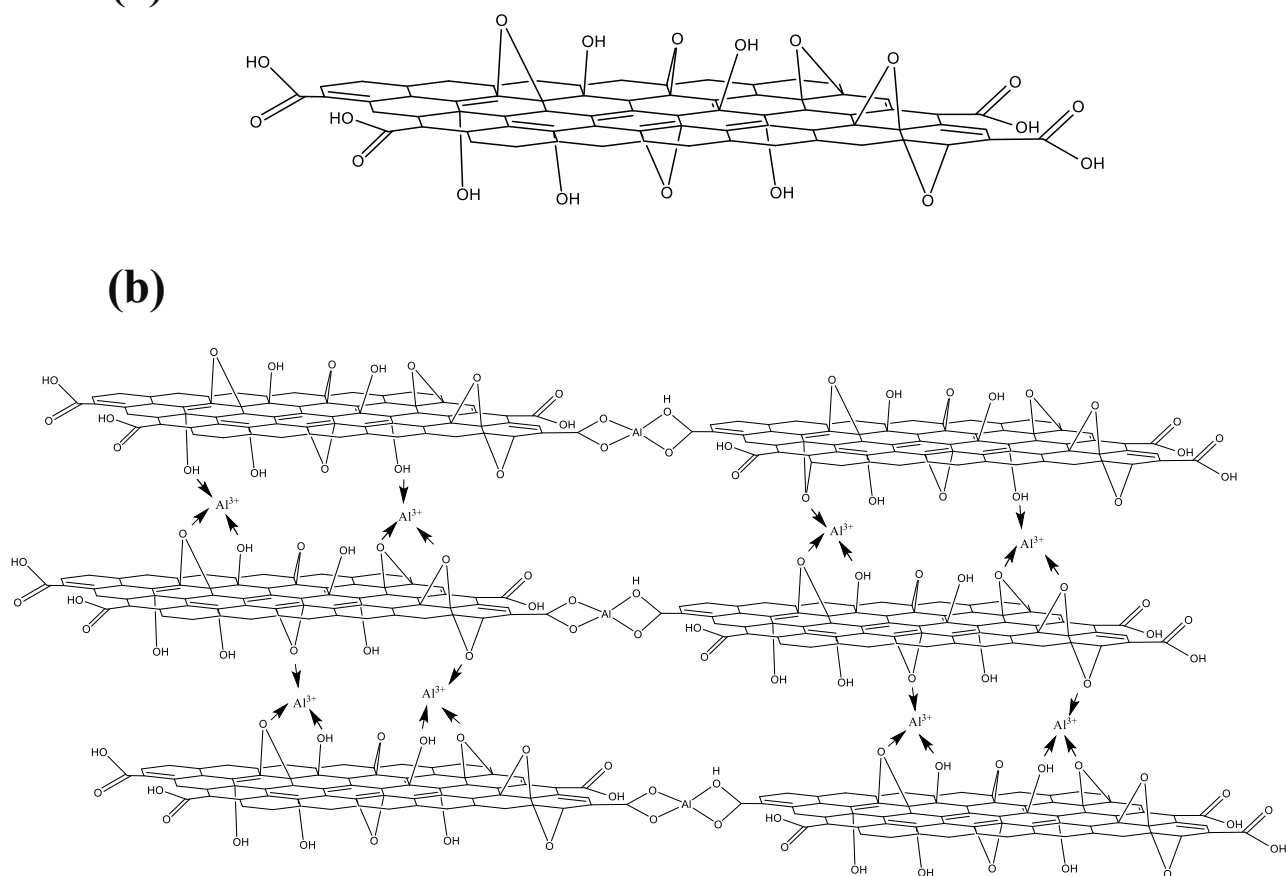
51 290

52 291 **CONCLUSIONS**

53
54
55
56 292 We successfully synthesized a new family of nonflammable, water-stable, flexible,
57
58 293 lightweight, and mechanically strong polymeric freestanding film of cl-GO, out of the highly
59
60 294 flammable, fragile and water-exfoliating GO. All experimental data consistently suggested the

1
2
3 295 cl-GO to possess such a microstructure as illustrated in Figure 7.
4
5
6 296

7
8 297
9
10 298
11
12 299
13
14 300
15
16
17 301
18
19
20
21
22
23
24
25
26
27
28
29
30
31
32
33
34
35
36



302 **Figure 7.** Illustration of cl-GO polymer's microstructure. a) GO; b) cl-GO.
37
38
39 303
40
41 304
42
43
44 305
45
46 306
47
48 307
49
50 308
51
52 309
53
54 310
55
56 311
57
58 311
59
60 312
313

This study confirmed the longstanding and so far not popularly known problem of the high flammability of the as-made GO from the modified Hummer's method, and developed a facile route to solving the problem that can otherwise dangerously jeopardize the large-scale production and applications of the graphene-related materials. Moreover in materials chemistry, the cross-linking method should be generally applicable to polymerizing many types of layered 2D-materials (e.g. h-BN, MoS₂, clays, etc.) and even nanocrystals, for meeting new challenge in tailor-making advanced materials at low-cost and high structural precision by design and on-demand.

314 **ASSOCIATED CONTENT**

315 **Supporting Information:** The following files are available free of charge. Videos from
316 exposing to open flame with the GO (S1.avi), and cl-GO (S2.avi).

317

318

319 **AUTHOR INFORMATION**320 **Corresponding Author**321 **Z. Ryan Tian**^{1,2,3*}322 **rtian@uark.edu**323 ¹Microelectronics/Photonics, University of Arkansas, Fayetteville AR 72701, USA324 ²Institute of Nanoscience/Engineering, University of Arkansas, Fayetteville AR 72701, USA325 ³Chemistry/Biochemistry, University of Arkansas, Fayetteville AR 72701, USA

326

327 **ACKNOWLEDGEMENT**

328 The authors acknowledges National Science Foundation- Experimental Program to Stimulate
329 Competitive Research (NSF-EPSCoR) for partial support, Prof. S. Yu's lab for the micro-
330 Raman experiments, and Dr. Jingyi Chen's lab for the TGA study.

331

332 **REFERENCES**

333 (1) Park, S.; Lee, K.-S.; Bozoklu, G.; Cai, W.; Nguyen, S. T.; Ruoff, R. S. Graphene Oxide
334 Papers Modified by Divalent Ions-Enhancing Mechanical Properties via Chemical
335 Cross-Linking. *ACS Nano* **2008**, *2*, 572–578.

336 (2) Frank, I. W.; Tanenbaum, D. M.; van der Zande, A. M.; McEuen, P. L. Mechanical
337 Properties of Suspended Graphene Sheets. *J. Vac. Sci. Technol. B Microelectron.*
338 *Nanom. Struct.* **2007**, *25*, 2558.

339 (3) Pacheco Sanjuan, A. A.; Wang, Z.; Imani, H. P.; Vanević, M.; Barraza-Lopez, S.
340 Graphene's Morphology and Electronic Properties from Discrete Differential

- 1
2
3 341 Geometry. *Phys. Rev. B* **2014**, *89*, 121403.
- 4
5 342 (4) White, C. T.; Li, J.; Gunlycke, D.; Mintmire, J. W. Hidden One-Electron Interactions in
6
7
8 343 Carbon Nanotubes Revealed in Graphene Nanostrips. *Nano Lett.* **2007**, *7*, 825–830.
- 9
10 344 (5) Pereira, J. M.; Vasilopoulos, P.; Peeters, F. M. Tunable Quantum Dots in Bilayer
11
12 345 Graphene. *Nano Lett.* **2007**, *7*, 946–949.
- 13
14
15 346 (6) Zhang, Y.; Tan, Y.-W.; Stormer, H. L.; Kim, P. Experimental Observation of the
16
17 347 Quantum Hall Effect and Berry’s Phase in Graphene. *Nature* **2005**, *438*, 201–204.
- 18
19 348 (7) van den Brink, J. Graphene: From Strength to Strength. *Nat. Nanotechnol.* **2007**, *2*,
20
21 349 199–201.
- 22
23
24 350 (8) Park, S.; Ruoff, R. S. Chemical Methods for the Production of Graphenes. *Nat.*
25
26 351 *Nanotechnol.* **2009**, *4*, 217–224.
- 27
28
29 352 (9) Kim, J.; Cote, L. J.; Kim, F.; Yuan, W.; Shull, K. R.; Huang, J. Graphene Oxide Sheets
30
31 353 at Interfaces. *J. Am. Chem. Soc.* **2010**, *132*, 8180–8186.
- 32
33
34 354 (10) Marcano, D. C.; Kosynkin, D. V; Berlin, J. M.; Sinitskii, A.; Sun, Z.; Slesarev, A.;
35
36 355 Alemany, L. B.; Lu, W.; Tour, J. M. Improved Synthesis of Graphene Oxide. *ACS*
37
38 356 *Nano* **2010**, *4*, 4806–4814.
- 39
40
41 357 (11) Huang, J.; Zhang, L.; Chen, B.; Ji, N.; Chen, F.; Zhang, Y.; Zhang, Z. Nanocomposites
42
43 358 of Size-Controlled Gold Nanoparticles and Graphene Oxide: Formation and
44
45 359 Applications in SERS and Catalysis. *Nanoscale* **2010**, *2*, 2733–2738.
- 46
47
48 360 (12) Xu, C.; Wang, X. Fabrication of Flexible Metal-Nanoparticle Films Using Graphene
49
50 361 Oxide Sheets as Substrates. *Small* **2009**, *5*, 2212–2217.
- 51
52
53 362 (13) Pham, T. A.; Kim, J. S.; Kim, J. S.; Jeong, Y. T. One-Step Reduction of Graphene
54
55 363 Oxide with L-Glutathione. *Colloids Surfaces A Physicochem. Eng. Asp.* **2011**, *384*,
56
57 364 543–548.
- 58
59
60 365 (14) Janowska, I.; Chizari, K.; Ersen, O.; Zafeiratos, S.; Soubane, D.; Costa, V. Da;
366 Speisser, V.; Boeglin, C.; Houllé, M.; Bégin, D.; *et al.* Microwave Synthesis of Large

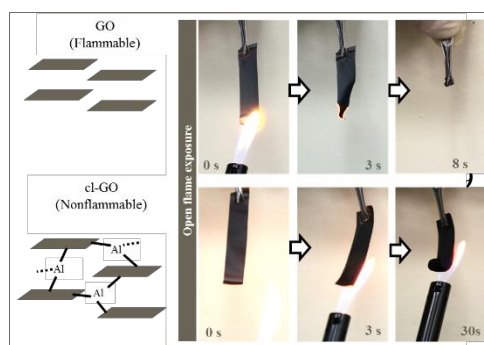
- 1
2
3 367 Few-Layer Graphene Sheets in Aqueous Solution of Ammonia. *Nano Res.* **2010**, *3*,
4
5 368 126–137.
6
7
8 369 (15) Kuila, T.; Mishra, A. K.; Khanra, P.; Kim, N. H.; Lee, J. H. Recent Advances in the
9
10 370 Efficient Reduction of Graphene Oxide and Its Application as Energy Storage
11
12 371 Electrode Materials. *Nanoscale* **2013**, *5*, 52–71.
13
14
15 372 (16) Mungse, H. P.; Verma, S.; Kumar, N.; Sain, B.; Khatri, O. P. Grafting of Oxo-
16
17 373 Vanadium Schiff Base on Graphene Nanosheets and Its Catalytic Activity for the
18
19 374 Oxidation of Alcohols. *J. Mater. Chem.* **2012**, *22*, 5427.
20
21
22 375 (17) Qiu, Y.; Collin, F.; Hurt, R. H.; Külaots, I. Thermochemistry and Kinetics of Graphite
23
24 376 Oxide Exothermic Decomposition for Safety in Large-Scale Storage and Processing.
25
26 377 *Carbon N. Y.* **2016**, *96*, 20–28.
27
28
29 378 (18) Kim, F.; Luo, J.; Cruz-Silva, R.; Cote, L. J.; Sohn, K.; Huang, J. Self-Propagating
30
31 379 Domino-like Reactions in Oxidized Graphite. *Adv. Funct. Mater.* **2010**, *20*, 2867–2873.
32
33
34 380 (19) Becerril, H. A.; Mao, J.; Liu, Z.; Stoltenberg, R. M.; Bao, Z.; Chen, Y. Evaluation of
35
36 381 Solution-Processed Reduced Graphene Oxide Films as Transparent Conductors. *ACS*
37
38 382 *Nano* **2008**, *2*, 463–470.
39
40
41 383 (20) Zhang, X.; Huang, Y.; Wang, Y.; Ma, Y.; Liu, Z.; Chen, Y. Synthesis and
42
43 384 Characterization of a graphene–C₆₀ Hybrid Material. *Carbon N. Y.* **2009**, *47*, 334–337.
44
45
46 385 (21) Krishnan, D.; Kim, F.; Luo, J.; Cruz-Silva, R.; Cote, L. J.; Jang, H. D.; Huang, J.
47
48 386 Energetic Graphene Oxide: Challenges and Opportunities. *Nano Today* **2012**, *7*, 137–
49
50 387 152.
51
52
53 388 (22) Hummers, W. S.; Offeman, R. E. Preparation of Graphitic Oxide. *J. Am. Chem. Soc.*
54
55 389 **1958**, *80*, 1339–1339.
56
57
58 390 (23) Lee, Y. R.; Kim, S. C.; Lee, H.; Jeong, H. M.; Raghu, A. V.; Reddy, K. R.; Kim, B. K.
59
60 391 Graphite Oxides as Effective Fire Retardants of Epoxy Resin. *Macromol. Res.* **2011**,
392 19, 66–71.

- 1
2
3 393 (24) Zhang, R.; Hu, Y.; Xu, J.; Fan, W.; Chen, Z.; Wang, Q. Preparation and Combustion
4
5 394 Properties of Flame Retardant Styrene-Butyl Acrylate Copolymer/Graphite Oxide
6
7
8 395 Nanocomposites. *Macromol. Mater. Eng.* **2004**, *289*, 355–359.
9
10 396 (25) Zhang, R.; Hu, Y.; Xu, J.; Fan, W.; Chen, Z. Flammability and Thermal Stability
11
12 397 Studies of Styrene-butyl Acrylate Copolymer/graphite Oxide Nanocomposite. *Polym.*
13
14 398 *Degrad. Stab.* **2004**, *85*, 583–588.
15
16
17 399 (26) Higginbotham, A. L.; Lomeda, J. R.; Morgan, A. B.; Tour, J. M. Graphite Oxide
18
19 400 Flame-Retardant Polymer Nanocomposites. *ACS Appl. Mater. Interfaces* **2009**, *1*,
20
21 401 2256–2261.
22
23
24 402 (27) Dasari, A.; Yu, Z.-Z.; Mai, Y.-W.; Cai, G.; Song, H. Roles of Graphite Oxide, Clay and
25
26 403 POSS during the Combustion of Polyamide 6. *Polymer (Guildf)*. **2009**, *50*, 1577–1587.
27
28
29 404 (28) Cui, W.; Guo, F.; Chen, J. Flame Retardancy and Toughening of High Impact
30
31 405 Polystyrene. *Polym. Compos.* **2007**, *28*, 551–559.
32
33
34 406 (29) Bajaj, P. Fire-Retardant Materials. *Bull. Mater. Sci.* **1992**, *15*, 67–76.
35
36 407 (30) Dikin, D. A.; Stankovich, S.; Zimney, E. J.; Piner, R. D.; Dommett, G. H. B.;
37
38 408 Evmenenko, G.; Nguyen, S. T.; Ruoff, R. S. Preparation and Characterization of
39
40 409 Graphene Oxide Paper. *Nature* **2007**, *448*, 457–460.
41
42
43 410 (31) Li, D.; Kaner, R. B. Materials Science. Graphene-Based Materials. *Science* **2008**, *320*,
44
45 411 1170–1171.
46
47
48 412 (32) Loh, K. P.; Bao, Q.; Eda, G.; Chhowalla, M. Graphene Oxide as a Chemically Tunable
49
50 413 Platform for Optical Applications. *Nat. Chem.* **2010**, *2*, 1015–1024.
51
52
53 414 (33) Eda, G.; Chhowalla, M. Chemically Derived Graphene Oxide: Towards Large-Area
54
55 415 Thin-Film Electronics and Optoelectronics. *Adv. Mater.* **2010**, *22*, 2392–2415.
56
57
58 416 (34) Zhu, Y.; James, D. K.; Tour, J. M. New Routes to Graphene, Graphene Oxide and
59
60 417 Their Related Applications. *Adv. Mater.* **2012**, *24*, 4924–4955.
418 (35) Kim, J.; Cote, L. J.; Huang, J. Two Dimensional Soft Material: New Faces of Graphene

- 1
2
3 419 Oxide. *Acc. Chem. Res.* **2012**, *45*, 1356–1364.
- 4
5 420 (36) Hu, M.; Mi, B. Layer-by-Layer Assembly of Graphene Oxide Membranes via
6
7 Electrostatic Interaction. *J. Memb. Sci.* **2014**, *469*, 80–87.
- 8 421
9
10 422 (37) Hung, W.-S.; Tsou, C.-H.; De Guzman, M.; An, Q.-F.; Liu, Y.-L.; Zhang, Y.-M.; Hu,
11
12 C.-C.; Lee, K.-R.; Lai, J.-Y. Cross-Linking with Diamine Monomers To Prepare
13 423
14 Composite Graphene Oxide-Framework Membranes with Varying D -Spacing. *Chem.*
15 424
16 *Mater.* **2014**, *26*, 2983–2990.
- 17 425
18
19 426 (38) Hu, M.; Mi, B. Enabling Graphene Oxide Nanosheets as Water Separation Membranes.
20
21
22 427 *Environ. Sci. Technol.* **2013**, *47*, 3715–3723.
- 23
24 428 (39) Han, Y.; Xu, Z.; Gao, C. Ultrathin Graphene Nanofiltration Membrane for Water
25
26 Purification. *Adv. Funct. Mater.* **2013**, *23*, 3693–3700.
- 27 429
28
29 430 (40) Yeh, C.-N.; Raidongia, K.; Shao, J.; Yang, Q.-H.; Huang, J. On the Origin of the
30
31 Stability of Graphene Oxide Membranes in Water. *Nat. Chem.* **2015**, *7*, 166–170.
- 32 431
33
34 432 (41) Tuinstra, F.; Koenig, J. L. Raman Spectrum of Graphite. *J. Chem. Phys.* **1970**, *53*,
35
36 433 1126–1130.
- 37
38 434 (42) Stankovich, S.; Dikin, D. A.; Piner, R. D.; Kohlhaas, K. A.; Kleinhammes, A.; Jia, Y.;
39
40 Wu, Y.; Nguyen, S. T.; Ruoff, R. S. Synthesis of Graphene-Based Nanosheets via
41 435
42 Chemical Reduction of Exfoliated Graphite Oxide. *Carbon N. Y.* **2007**, *45*, 1558–1565.
- 43 436
44
45 437 (43) Fan, Z.; Wang, K.; Wei, T.; Yan, J.; Song, L.; Shao, B. An Environmentally Friendly
46
47 and Efficient Route for the Reduction of Graphene Oxide by Aluminum Powder.
48 438
49
50 439 *Carbon*, *2010*, *48*, 1686–1689.
- 51
52
53 440 (44) Yang, D.; Velamakanni, A.; Bozoklu, G.; Park, S.; Stoller, M.; Piner, R. D.;
54
55 Stankovich, S.; Jung, I.; Field, D. A.; Ventrice, C. A.; *et al.* Chemical Analysis of
56 441
57 Graphene Oxide Films after Heat and Chemical Treatments by X-Ray Photoelectron
58 442
59 and Micro-Raman Spectroscopy. *Carbon N. Y.* **2009**, *47*, 145–152.
- 60 443
444 (45) Cristina Gómez-Navarro, †; R. Thomas Weitz, †; Alexander M. Bittner, †; Matteo

- 1
2
3 445 Scolari, ‡; Alf Mews, ‡; Marko Burghard, *, † and; Klaus Kern†, §. Electronic
4
5
6 446 Transport Properties of Individual Chemically Reduced Graphene Oxide Sheets. **2007**.
7
8 447 (46) Eda, G.; Fanchini, G.; Chhowalla, M. Large-Area Ultrathin Films of Reduced
9
10 448 Graphene Oxide as a Transparent and Flexible Electronic Material. *Nat. Nanotechnol.*
11
12 449 **2008**, 3, 270–274.
13
14
15 450 (47) Wang, X.; Jiao, L.; Sheng, K.; Li, C.; Dai, L.; Shi, G. Solution-Processable Graphene
16
17 451 Nanomeshes with Controlled Pore Structures. *Sci. Rep.* **2013**, 3, 1996.
18
19
20 452

21
22 **TOC Graphic**
23
24



464